Additive Manufacturing 23 (2018) 355–361

Contents lists available at ScienceDirect

Additive Manufacturing

journal homepage: www.elsevier.com/locate/addma

Full Length Article

A new photopolymer extrusion 5-axis 3D printer

Muhammad Asif[a,b], Joo Hyun Lee[c], Mikyla J. Lin-Yip[c], Simone Chiang[c], Alexis Levaslot[d], Tim Giffney[c], Maziar Ramezani[a], Kean Chin Aw[c,*]

[a] Mechanical Engineering, Auckland University of Technology, Auckland, New Zealand
[b] Department of Engineering Sciences, PNEC, National University of Science and Technology, Islamabad, Pakistan
[c] Mechanical Engineering, University of Auckland, Auckland, New Zealand
[d] Department of Materials Engineering, Ecole Nationale Supérieure d'Ingénieurs de Caen, France

ARTICLE INFO

Keywords:
Photopolymer
Extrusion
Free-form structures
3D printing

ABSTRACT

Popular 3D printing techniques such as fused deposition modelling (FDM) and stereolithography (SLA) have certain limitations and challenges. Although printing multi-material functional parts combining smart and conventional materials is a promising area, existing printers are not ideally suited to this, with FDM printers typically requiring high operating temperatures and SLA using a tank containing one single material. Common 3D printers also require the deposition of additional "support" material to hold the shape of an object when printing overhang structures. The concept of adding additional rotational axes to the system to eliminate this problem has shown promising results, but such systems still lack the capability to print complex structures without supports. To overcome these limitations there is a need to develop a new 3D printing techniques that combine the strengths of existing methods. A photopolymer extrusion 3D printing technique, which combines the strengths of FDM and UV assisted 3D printing technology is demonstrated in this paper. By using photopolymer extrusion in combination with two additional rotational axes, the printer developed in this work not only allows the traditional layer upon layer printing, but is also capable of free form printing. Fumed silica is used as a filler in order to control the material viscosity for proper extrusion and curing. Mechanical tests were conducted on objects printed using different concentrations of filler in the photopolymer to understand its effect and determine the range of suitable filler concentration. Then, printing of free-form and self-supported structures is successfully demonstrated.

1. Introduction

3D printing is a useful technique for manufacturing mechanical parts, with several advantages including freedom to fabricate intricate geometries, lack of material waste, and elimination of expensive tooling [1]. Particularly when the number of parts required is small, 3D printing techniques can help to avoid high setup costs, as well as reducing manufacturing time [2]. Although it might take up to several hours or even days to manufacture an object, this is still a short total time to obtain a physical product from a CAD file. Various 3D printing technologies such as fused deposition modelling (FDM) [3], stereolithography (SLA) [4], selective laser sintering (SLS) [5], and the binder jet technique [6] have been developed. Each technique has different capabilities for the material(s), size, complexity, and geometry of the printed objects, as well as different ability to deposit support material layer-by-layer and print overhanging or bridging structures. However, the construction of self-supporting [7] 3D freeform structures (e.g. a helix) without requiring support material remains a big challenge [8,9]. Additionally, multi-material 3D printing is increasingly desirable to allow functional parts combining materials of different mechanical properties, or even integrated sensors, to be produced [10,11]. A technology well suited to multi material printing that avoids the high temperatures of FDM and single material bath of SLA is therefore desired.

Ideally, a 3D printer should be able to produce parts of any desired geometry. In practice, it is challenging to produce overhanging or bridging structures due to the effect of gravity on the softened material (in FDM) or wiping action between layers (in SLA). Until now, this difficulty has been addressed by generating additional "support" material to prevent overhanging elements of the printed structure from sagging until it is solidified or cured. The requirement for these supports is a significant drawback due to the increased production time and material wastage. Removing support material after curing may be difficult (e.g. internal supports in a tube or cavity) or leave damage or

* Corresponding author.
E-mail address: k.aw@auckland.ac.nz (K.C. Aw).

https://doi.org/10.1016/j.addma.2018.08.026
Received 7 June 2018; Received in revised form 20 August 2018; Accepted 24 August 2018
Available online 25 August 2018
2214-8604/

marks on the part surface. Methods to allow printing of complex structures without support are therefore desired.

While FDM has sometimes been used to print free-from micro-structures, this technique has some shortcomings: as the material is a thermoplastic, it can be softened by heat during the remainder of the printing process, with deformation of the extruded material during the cooling and hardening stage making it difficult to achieve accurate geometry without support material [12].

Photopolymer extrusion is a more promising technique for printing freeform structures e.g. by ultraviolet light assisted 3D printing (UV-3DP) [12] and direct-print photopolymerization [14]. Both of these examples use a syringe driver to extrude the material, with the drawback of small reservoir size meaning that this method is effective for small test parts only. In addition, these photopolymer extrusion techniques have a conventional 3-axis layout. Even using photopolymer extrusion, it is difficult to print complex free-form structures with a 3-axis machine.

5-axis printing has advantages for printing complex structures. Optomec Inc. has developed a 3D printer that implements a 5 axes system to print electronics onto complex 3D surfaces [15]. It has a print envelope of 200 mm × 300 mm × 200 mm, and has the capability to print features from 10 μm to 1 mm. Despite utilising a 5 axis system, the printer is still limited to a layer by layer technique as the technology involves high velocity deposition. The materials are volatile, hard to handle, and sensitive to the environment. Another 3D printer that utilises a 5-axis system has been developed by a team of The Welding Institute (TWI) under the MERLIN project using laser metal deposition methodology [16]. The principle of this technology is based on SLS and laser cladding. The technology is still a layer by layer method, and it is unavoidable to build a supporting platform that is difficult to disconnect due to strong bonding between welded components. The most recent research that integrates additional axes to a 3D printer system uses the FDM technique and has been conducted by the University of Oslo. The printer has a fixed XZ plane motion on the print head, two rotational axes and the Y-axis are attached to the print bed. With a fixed nozzle head, it limits tool pathing while printing complex structures. Gravitational factors need to be considered if the object is tilted during the printing process [17].

A move from 3-axis to 5-axis printing has another potential advantage. Existing 3D printers usually produce objects in a strict layer by layer fashion. While this substantially simplifies tool path generation, the mechanical properties of printed structures may depend on the orientation of the slicing plane [6]. In particular, a part that has been printed layer by layer is likely to have different strength along and between the slice planes. Combined with appropriate tool path generation, a 5-axis printer could deposit material in a wider range of directions allowing for the strength of a part in various directions to be customised. Whereas, the method of using additional axes to the system is increasing nowadays, these axes are all rotational axes to allow either the tools or build platform to accommodate the movements in the space. By using this method, complex free-from and self-supported 3D structures can be printed more accurately and in less time.

To overcome the limitations discussed above there is a need to develop new 3D printing methods that combine the strengths of existing techniques and fully realise printing of free-form, self-supported 3D structures. Both a printing technique where deposited material can be permanently cured so as to be self-supporting, and a machine layout that allows complex extrusion paths, must be combined in one device. Printing of macroscopic objects with a high level of detail will also require a material extrusion system that can precisely control the deposited volume independent of the total size of the part (unlike a syringe driver). Ideally, deposition of a range of materials will be possible, without requiring feed materials to be diluted with a solvent (that would otherwise reduce the speed and efficiency of producing bulk objects).

2. Methods and materials

Our proposed system is a hybrid of FDM and UV assisted 3D printing technologies, which combines FDM-style extrusion from a nozzle with UV curing, and implements 5 axis movement for printing of complex structures. The combination of photopolymer extrusion with the integration of two additional rotational axes on the extruder allows various free-form and self-supported 3D structures to be printed easily. With these additional two degrees of freedom the extruder can maintain the proper angle relationship between the extrusion nozzle and the deposited material even while following a complex motion path, improving the ability of our system to print true free-form and self-supported structures. A positive displacement peristaltic pump is applied to precisely control the amount of material extruded. This approach has the advantage that the precision at which the volume of deposited material can be controlled does not depend on the amount of material in the reservoir.

This hybrid 3D printer extrudes photopolymer in a similar configuration to an FDM printer. Photopolymer resin is deposited from an extrusion nozzle that is attached to a 5-axis motion system. The extruded photopolymer can then be cured solid soon after leaving the nozzle upon exposure to ultraviolet (UV) light from UV laser diodes that move with the printing nozzle. Two rotational axes (A, B) along with the Cartesian axes (X, Y, Z) allow freeform printing in addition to conventional layer by layer printing. As this printing technique does not require a material bath, works at low temperature, and can print more viscous materials than an inkjet printing head, it is suitable for future printing of multi material structures.

To customize the properties of the deposited material during printing and the mechanical properties of the finished part after curing, fillers were added into the photopolymer resin. The effect of adding different concentrations of fumed silica as filler on the viscosity of the deposited liquid and the strength and dimensional accuracy of the finished parts is investigated to provide a starting point for producing mechanical parts using the developed technique.

2.1. A new photopolymer extrusion 5-axes printer

Fig. 1 shows the 5-axis photopolymer extrusion (PPE) printing technique. The entire 3D printing system includes the UV curing system based on two UV laser diodes, an extrusion system consisting of the stationary peristaltic pump, flexible tubing, and the extrusion nozzle, and a platform with 3 linear motions (X, Y and Z) and 2 rotary motions (A and B).

Fig. 2 shows a picture of the PPE printer showing the 5 axes and a close-up of the nozzle with laser diodes mounted on each side.

All axes can be controlled simultaneously for continuous adjustment

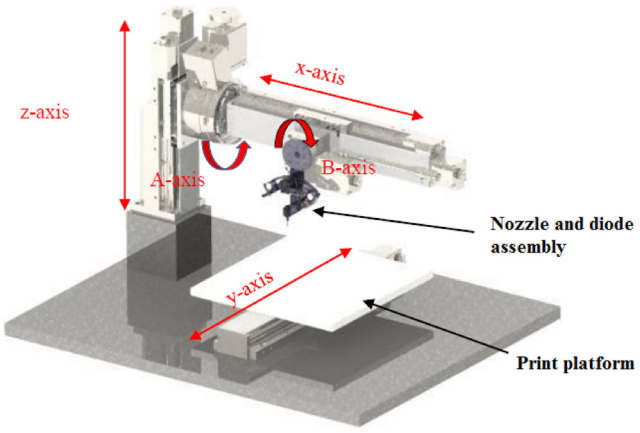

Fig. 1. A schematic of the 5 axes photopolymer extrusion printer.

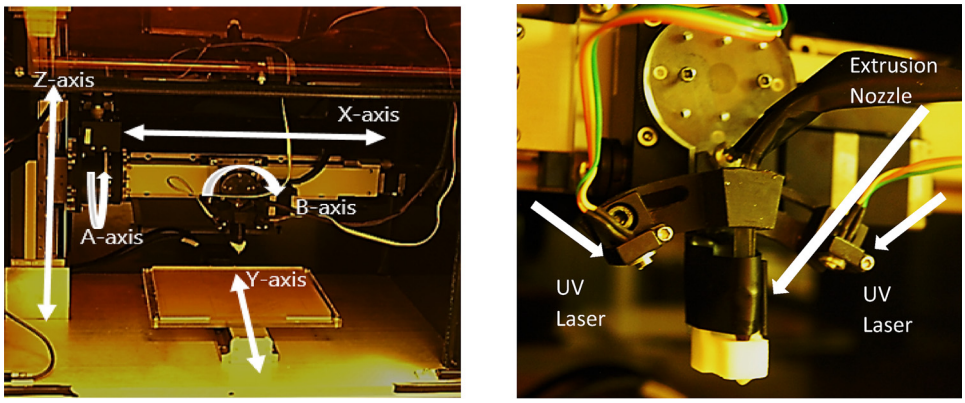

Fig. 2. (a): 5-axis PPE printer (b) UV laser and extrusion nozzle.

of the nozzle angle and position while printing complex objects. Most importantly, the 2 additional rotational axes are implemented by mounting rotational motors on the built platform. These 2 additional rotational axes (A and B) provide better printing of free-form and free standing objects (for example a helical object). By having more degrees of freedom, the extrusion nozzle has the ability to move in a more complex path providing the ability to print much more complex objects.

As the aim of the system is to print complex free standing and free-form structures, the extrusion system must be capable of delivering a precise amount of fluid in small quantities and have sufficient power to push the viscous fluid through the nozzle. Deposition should be done through a small nozzle tip to control its output, a 21 gauge (0.51 mm) nozzle is used in this study. A pair of peristaltic pumps is used to deliver the photopolymer blend from a reservoir to an extrusion nozzle. In comparison to the common use of syringe drivers [13,14], the size of the material reservoir is not related to the smallest volume increment that can be dispensed enabling multi-scale printing. An Arduino microcontroller [15] and the open source host software Pronterface [16] control the machine. The entire equipment is enclosed in a UV-opaque case to prevent unwanted curing of the resin from ambient white light, and protect the operator from laser radiation.

The UV curing system uses two UV laser diodes placed around the extrusion head to provide even curing of the extruded photopolymer. The purpose of using UV laser as curing source is to focus on the deposited polymer without affecting surrounding material. The lasers have an output power of 40 mW with a wavelength of 405 nm (Thorlabs DL5146-101S) [17] which can rapidly cure the resin. The laser beams have an elliptical profile with beam divergence of 8 degrees in the narrow axis of the ellipse and perpendicular divergence of 19 degrees in the long axis of ellipse.

2.2. Preparation of UV curable resin

The photopolymer resin (UV Dome 58) being extruded was commercially procured from Whitehall Technical Services Ltd, Auckland, New Zealand. It is based on a proprietary epoxy acrylate that is designed to be cured with UV exposure at 405 nm. Fillers due to their high stiffness can be used to diversify and improve mechanical properties [18]. In this study, fumed silica is added to the resin. The fumed silica is used to control the fluid viscosity and may be useful for increasing the mechanical properties [18]. Fumed silica has nanoparticles with a very large surface area and a low bulk density. Before mixing, it is in the form of a white powder. The powder is very lightweight and insoluble with water. With adequate homogenization, it is possible to mix the fumed silica particles can be mixed into other components of the resin. Adding silica changes the rheological behaviour of the resin, adjusting the viscosity of the fluid [19]. As shown in Fig. 3, the fumed silica

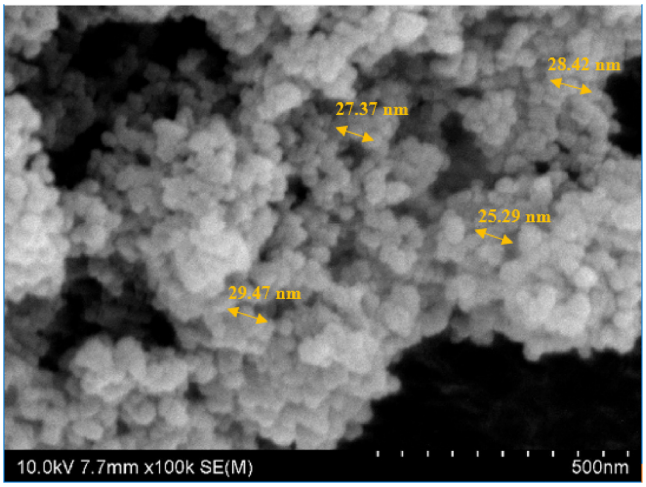

Fig. 3. SEM image of the fumed silica nanoparticles.

nanoparticles have a spherical shape with diameters ranging approximately between 25 to 30 nm. The particles make up long chains or form agglomerates. The diameter of agglomerates depends on the interaction conditions when the particles are mixed with the resin.

To investigate the mechanical properties of printed parts, samples were prepared with different concentrations of the silica filler (by weight) mixed into the resin. Mixtures were prepared the same day to have samples with the same aging and were prepared inside a room with UV-free illumination to avoid premature curing. A total of 100 g of mixture was made for each concentration, for instance for a mixture with 2% filler by weight, 98 g of the resin was mixed with 2.0 g of fumed silica. After a slow manual stirring for 5–10 min with a thin spatula, the mixture was treated with an ultrasonic homogenizer. The Sonics and Materials Inc ultrasonic homogenizer [20] was applied for 2 periods of 1 min at 20 kHz of ultrasound frequency and 130 W of intensity. Finally, to remove air bubbles from the mixture, the samples were degassed in a vacuum oven for 45 min at 65 °C.

3. Results and discussion

The key parameters for the material (such as filler concentration) and printing process (such as extrusion rate) were investigated to observe their effects on the dimensional accuracy and mechanical strength of the printed objects.

3.1. Effect of filler on material viscosity

In order to obtain smooth extrusion, the viscosity of the resin must lie within a certain range. If the viscosity of the resin is low, it is likely to spread due to gravity before it can be cured by the UV laser, but if the viscosity is high, it will be difficult to extrude the resin through the nozzle. Therefore, the resin viscosity was measured with different filler concentrations using a rheometer and their printability was observed.

Resins with 2%, 4%, 6%, 8%, 10%, and 12% of fumed silica by weight were prepared as per Section 2.2. The dynamic viscosity of each concentration was measured using a rheometer (Brookfield Ltd DV3T Extra).

The rheometer drives a spindle immersed in the fluid to be tested, through a calibrated spring. The user gives a constant rotational speed value (rpm) to the spindle and the fluid, inside a stationary cylinder container. The viscous drag created by the rotational force (or moment force or torque: τ) against the spindle is measured by the spring system.

In order to accurately measure the viscosity of resin with the concentrations of fumed silica mentioned above a 64 gauge spindle was used. For each sample the revolution speed was adjusted to achieve a torque close to the midpoint (50%) of the sensor range. The rheometer then calculates a viscosity value based on the spindle, speed, and measured torque. Table 1 lists the parameters used and the measured viscosity.

Higher viscosity can cause difficulties during printing, resulting with inconsistent extrusion, while low viscosity results with the composite not being able to stay in shape while being cured by the pulsed UV beam. Therefore, defining an appropriate range of viscosity to extrude the composite from the deposition nozzle is very important. As shown in Fig. 4, dynamic viscosity increases substantially with increasing percentage of filler. Fillers up to 6% were found to have low viscosity, while viscosity increased rapidly for filler concentrations greater than 9%. With the printer using a 21 gauge (0.5 mm) nozzle, only a narrow window of filler concentrations of 8% and 9% (corresponding to the dynamic viscosities of 15,000 cP and 17,000 cP) were found to be suitable to print reliably.

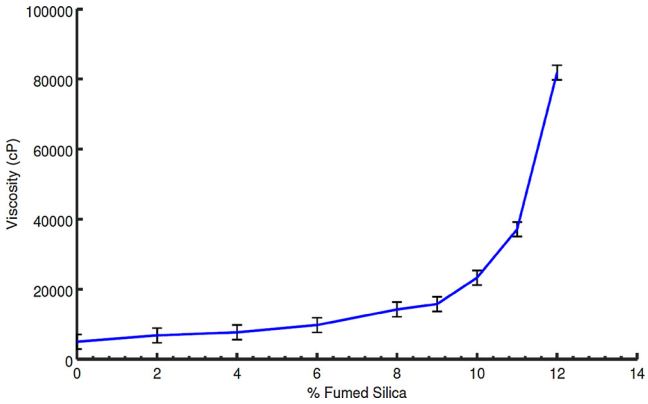

Fig. 4. Effect of filler concentration on dynamic viscosity.

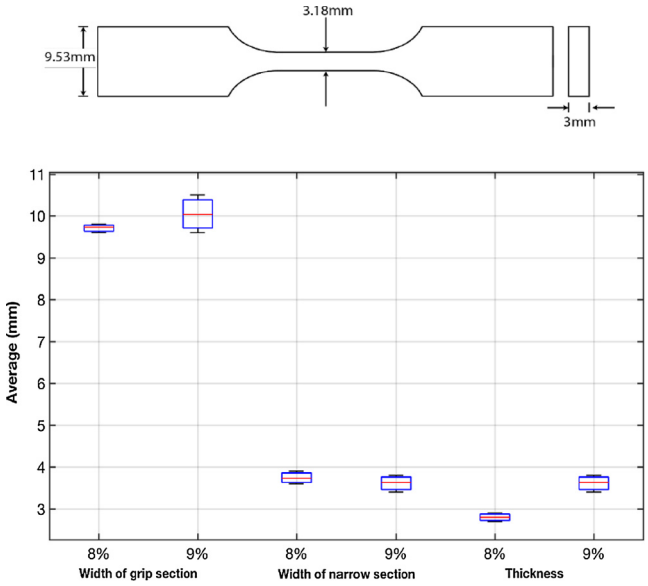

Fig. 5. Comparison between designed and printed dimensions.

3.2. Effect of filler on dimensional accuracy

The aim of dimensional accuracy measurement was to study the effect of filler on printed dimensions; ideally printed dimensions should closely follow the CAD model dimensions. In this work, the printed dimensions; i.e. width (at two ends) and thickness were taken into account, with CAD model as the benchmark. Fig. 5 presents the average and deviation of the printed dimensions of width (at two positions) and thickness of samples printed with 8% and 9% filler concentrations. Three samples were printed and measured for each filler concentration. From Fig. 5, the variation in the printed dimensions are slightly higher in 9% filler samples. The thickness of 9% filler sample is higher as the uncured material with this high filler percentage has higher viscosity; hence less sideways spreading than 8% filler samples. Higher filler concentration may lead to more deviation in the printed dimensions as it is difficult to extrude from the deposition nozzle due higher viscosity. Hence, the printed part could vary from the targeted dimension and obtaining a part with very high dimensional accuracy is often not possible.

3.3. Effect of filler on mechanical properties

In order to test the strength and quality of the printed objects, dog-bone samples of specific dimensions (following ASTM D638 standard type V as shown in Fig. 6) were 3D printed. Tensile and 3-point bending

Table 1
Parameters and measured viscosity.

Filler Concentration (%)	Spindle	Speed (rpm)	Torque (%)	Time (s)	Viscosity (cP)	Viscosity (Pa.s)
0	64	50	50.4	36	6048	6.05
2	64	40	50.3	35	7545	7.54
4	64	38	52.5	37	8289	8.29
6	64	35	58.1	58	9960	9.96
8	64	21	52	30	14860	14.9
9	64	18	50.7	33	16900	16.9
10	64	12	50	33	25000	25
11	64	10	59.5	41	35700	35.7
12	64	4	53.2	32	79800	79.8

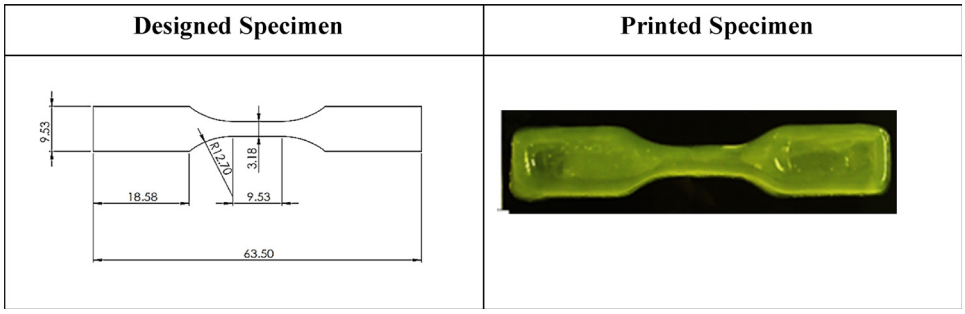

Fig. 6. Designed and fabricated specimen.

tests were conducted on these samples to characterize tensile strength, young's modulus, strain at break and flexural strength.

3.3.1. Tensile test

Improved mechanical properties e.g. tensile strength and Young's modulus may be achieved by optimizing the filler loading due to increase in weight fraction or volume fraction leading to a continuous and uniform interface, which creates a strong polymer network [21]. A large amount of research has been conducted on different polymer nanocomposites in order to study the effect of weight fraction and volume fraction (%) on mechanical properties of polymer nanocomposites [21–26]. In an attempt to understand the effect of weight fraction of silica nanoparticles on mechanical properties of epoxy, Liu et al. calibrated Young's modulus and tensile stress at different weight fractions [22]. They reported gradual increase in both Young's modulus and tensile stress with an increase in weight fraction of silica nanoparticles. Other studies have also been conducted on the effect of different weight fractions of silica nano-particles on tensile stress and Young's modulus of epoxy resin [21,27]. They found that value of Young's modulus and yield stress of epoxy-silica nanocomposite at 20% weight fraction are 1.22 and 1.28 times the value of pure epoxy [27].

In order to study the effect of our chosen filler on mechanical properties of our nanocomposite, resin with 8% and 9% silica nanoparticles were used. Six pieces for each concentration were printed. The tensile and flexural strengths were then determined from tensile and 3-point bending tests respectively.

Fig. 7 shows the stress-strain diagram representative of 2 different filler concentrations. It is quite evident from the stress-strain diagram that samples printed by 8% filler have higher strain at break, while the samples printed with 9% filler have higher yield stress. Table 1 shows the tensile properties of samples with 8% and 9% filler concentration. It indicates that higher filler percentage made the samples less elastic.

As shown in Table 3, significant increase in the Young's modulus is observed with increasing the filler content, suggesting efficient transfer of stresses via interface and high interfacial stiffness. Due to the high rigidity of silica nanoparticles, tensile strength and Young's modulus of the particulate nanocomposite is increased with increasing the filler content compared with the neat resin. It was found that the average tensile strength of 8% and 9% filler concentrations is 4.13 and 4.26 times and average Young's modulus is 6.68 and 8.13 times the value of neat resin respectively. As the standard deviations shown in Table 3 are not high in comparison to the difference between the averages of the sample groups, the experimental results are reasonably significant.

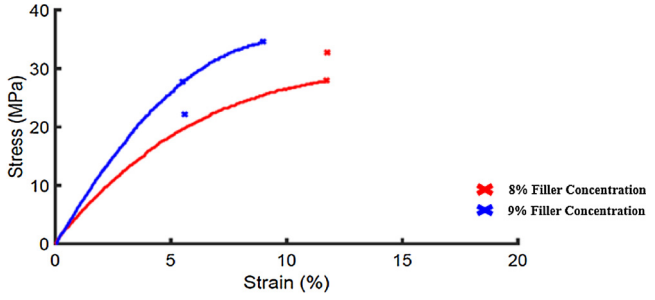

Fig. 7. Tensile stress-Strain diagram.

3.3.2. Flexural test

Researchers have reported the flexural properties of silica nanocomposites e.g. Hsiao et al. [28] reported flexural strength of ductile and brittle matrix epoxy-silica nanocomposite and observed linear increase in flexural strength with increase in particle loading.

A 3-point test was used to determine the flexural properties of the printed objects with 8% and 9% filler. Table 4 summarizes the results of the 3-point tests. As summarized in Table 2, the increase in flexural strength of nanocomposite compared with neat resin is due to the silica nanoparticles. Both concentrations 8% and 9% found to have nearly the same flexural strength. Again, it shows that higher percentage of filler makes the sample slightly more brittle.

3.4. Free-form and self supported structures

The basic capability of printing free-from and self-supported structures using this 5-axes extrusion printer was demonstrated, including exploiting the two rotational axes A and B. Since there is no available translational algorithm to convert the CAD model into a free-from printing path, the printing of free-from and self-supported structures is controlled through manually generated G-code. As this is in the preliminary development stage, the demonstrated free-form structures will be limited.

Fig. 8 shows the printing of a self-supporting staircase shape object. This is done by moving the x, y, z and B axes. Fig. 8 shows how the fourth axis; i.e. the B-rotational axis is turned by 30° with respect to the z-axis, when the horizontal traces are being printed.

The staircase objects in Fig. 9 show the progression of altered printing parameters. The printed staircase objects has the first step height of 20 mm, and subsequent steps are 10 mm tall. The difference between the models in Fig. 9(a)–(c) are varying feed rates for motion in the z- and x-directions, as well as when rotating, and varying extrusion rates.

Table 5 shows that the printing parameters corresponding to

Table 2
Process parameters for 8% and 9% samples.

Process Parameters	Variables		
Print Setting	Layers and Perimeters	*Layer height (mm)*	3.22
		First layer height (mm)	0.20
	Infill	*Fill density (%)*	40
	Speed (print moves)	*Perimeters (mm/s)*	20
		Infill (mm/s)	40
	Overall Time/Sample	*(min)*	10
Filament Setting	Filament	*diameter (mm)*	1
	Extrusion	*Extrusion multiplier*	0.0055

Table 3
Mechanical properties of 8% and 9% filler concentration.

Filler Concentration (%)	Average Ultimate Tensile Strength (MPa)	Standard Deviation (UTS)	Average Young's Modulus (MPa)	Standard Deviation (Young's Modulus)	Average Yield (MPa)	Standard Deviation (Yield)	Average Strain at Break (%)	Standard Deviation (Strain at Break)
8	30.2	3.1	478.5	79.9	13.9	2.1	15.0	4.7
9	31.1	4.9	582.3	65.3	15.8	3.1	7.1	2.4

Table 4
Flexural properties of 8% and 9% filler concentrations.

Filler Concentration (%)	Average F_{max} (N)	Standard Deviation (F_{max})	Average Max deflection before break (mm)	Standard Deviation (Max deflection before break)	Average Flexural Strength (MPa)	Standard Deviation (Flexural Strength)
8	16.3	0.8	8.5	2.1	18.8	1.4
9	14.6	0.8	7.9	1.3	18.4	1.0

Fig. 8. Diagram indicating nozzle orientation (B-axis) for printing vertical and horizontal sections of the staircase object.

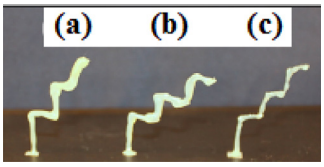

Fig. 9. Staircase printed models. a) Extrusion is too high. b) Too slow rotation feed rate, c) Smaller extrusion but faster feed rate.

Table 5
Printing parameters for Fig. 9(c).

S.No	Printing Parameters	Value
1	Vertical Feed Rate	21 mm/min
2	Horizontal Feed Rate	19 mm/min
3	Extrusion	1.4 mm/min
4	Rotation Angle (B-Axis)	30°
5	Laser Angle	40°

Fig. 9(c) providing relatively better dimensional accuracy.

Finally, to demonstrate the 5 axes capability of the printer to print a self-supporting and free form structure, a horizontal U-shape was printed as shown in Fig. 10. This requires all the x, y, z, A and B axes to move. The nozzle has its B-axis tilted to 45° (along y-axis) with respect to the z-axis when it travels at the bend and then reduces slightly to 30° while tilting the A-axis to 10° (along x-axis) with respect to the z-axis as it travels to the right. As the nozzle travels along the U-bend, the B-axis

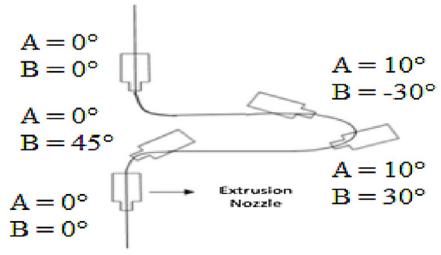

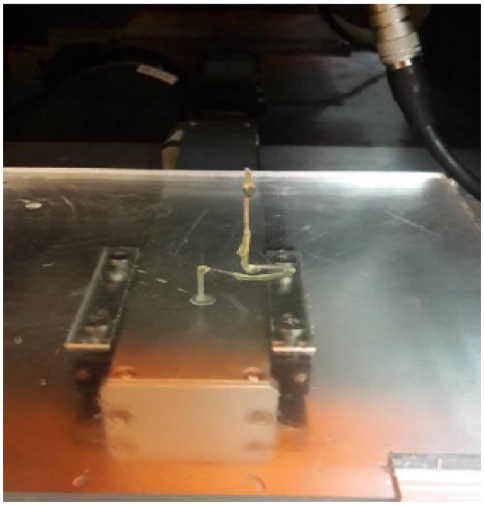

Fig. 10. Free-form horizontal U-shape.

is being tilted in steps to −30°. Then the nozzle will return the A-axis angle to 0° and B-axis 45° when travelling to the left. Finally both A and B axes will change to 0° to print the vertical trace. Blobs were formed during the printing process when the angle of A or B changes and to eliminate these blobs and ensure consistent diameter throughout the print, a better control of the polymer extrusion is required in the future. However, this preliminary demonstration has showed the capability of the 5-axis PPE printer to print free-form structures.

4. Conclusions

A 5-axis photopolymer extrusion 3D printer has been developed and tested. The system extrudes UV-curable resin through a nozzle moving in free space, while rapidly curing the deposited material using UV diode lasers. Because the nozzle can be rotated around two axes to approach a point in space from the desired angle, and the UV lasers cure

the photopolymer resin quickly as it leaves the nozzle, the method is suitable for printing of freeform structures. To reinforce the resin, and achieve proper viscosity for proper extrusion, fumed silica is added to the uncured resin to form a composite. The fumed silica content helps ensure that the extruded resin stays in form long enough to be cured through UV exposure without flowing. 8%–9% filler concentration was found to be suitable with the current nozzle size. Dog bone samples were printed to investigate whether adding filler in the photopolymer have any effect on mechanical properties and dimensional accuracy of the printed parts. The strength of the fabricated parts was measured through tensile and flexural tests. Although we have demonstrated a system capable of printing self-supporting and free-form structures, future work will be required to improve the smoothness and accuracy of the printed objects. Also, automated software (comparable in function to the slicing software for conventional 3D printing) to generate and optimize the complex 5-axis printing path is required and is an on-going research concern.

References

[1] H.K. Rafi, N.V. Karthik, H. Gong, T.L. Starr, B.E. Stucker, Microstructures and mechanical properties of Ti6Al4V parts fabricated by selective laser melting and electron beam melting, J. Mater. Eng. Perform. 22 (2013) 3872–3883, https://doi.org/10.1007/s11665-013-0658-0.

[2] W.E. Frazier, Metal additive manufacturing: a review, J. Mater. Eng. Perform. 23 (2014) 1917–1928, https://doi.org/10.1007/s11665-014-0958-z.

[3] I. Zein, D.W. Hutmacher, K.C. Tan, S.H. Teoh, Fused deposition modeling of novel scaffold architectures for tissue engineering applications, Biomaterials 23 (2002) 1169–1185, https://doi.org/10.1016/S0142-9612(01)00232-0.

[4] H.N. Chia, B.M. Wu, Recent advances in 3D printing of biomaterials, J. Biol. Eng. 9 (2015).

[5] O.A.M. Abdelaal, S.M.H. Darwish, Review of Rapid prototyping techniques for tissue engineering scaffolds fabrication, in: A. Öchsner, L.F.M. da Silva, H. Altenbach (Eds.), Charact. Dev. Biosyst. Biomater. Springer Berlin Heidelberg, Berlin, Heidelberg, 2013, pp. 33–54, , https://doi.org/10.1007/978-3-642-31470-4_3.

[6] M.P. Chae, W.M. Rozen, P.G. McMenamin, M.W. Findlay, R.T. Spychal, D.J. Hunter-Smith, Emerging applications of bedside 3D printing in plastic surgery, Front. Surg. 2 (2015) 25.

[7] K.F. Leong, C.M. Cheah, C.K. Chua, Solid freeform fabrication of three-dimensional scaffolds for engineering replacement tissues and organs, Biomaterials 24 (2003) 2363–2378.

[8] C. Ladd, J.H. So, J. Muth, M.D. Dickey, 3D printing of free standing liquid metal microstructures, Adv. Mater. 25 (2013) 5081–5085, https://doi.org/10.1002/adma.201301400.

[9] R. Engelke, G. Engelmann, G. Gruetzner, M. Heinrich, M. Kubenz, H. Mischke, Complete 3D UV microfabrication technology on strongly sloping topography substrates using epoxy photoresist SU-8, Microelectron. Eng. 73–74 (2004) 456–462, https://doi.org/10.1016/j.mee.2004.03.017.

[10] J. Rossiter, P. Walters, B. Stoimenov, Printing 3D Dielectric Elastomer Actuators for Soft Robotics, (2009), https://doi.org/10.1117/12.815746 72870H–72870H–10.

[11] D. Raviv, W. Zhao, C. McKnelly, A. Papadopoulou, A. Kadambi, B. Shi, S. Hirsch, D. Dikovsky, M. Zyracki, C. Olguin, R. Raskar, S. Tibbits, Active Printed Materials for Complex Self-Evolving Deformations vol. 4, (2014), p. 7422, https://doi.org/10.1038/srep07422 http://dharmasastra.live.cf.private.springer.com/articles/srep07422#supplementary-information.

[12] Y. Akira, N. Fuminori, I. Koji, A three-dimensional microfabrication system for biodegradable polymers with high resolution and biocompatibility, J. Micromech. Microeng. 18 (2008) 25035 http://stacks.iop.org/0960-1317/18/i=2/a=025035.

[13] G. Vozzi, A. Previti, D. De Rossi, A. Ahluwalia, Microsyringe-based deposition of two-dimensional and three-dimensional polymer scaffolds with a well-defined geometry for application to tissue engineering, Tissue Eng. 8 (2002) 1089–1098, https://doi.org/10.1089/107632702320934182.

[14] M. Vlasea, E. Toyserkani, Experimental characterization and numerical modeling of a micro-syringe deposition system for dispensing sacrificial photopolymers on particulate ceramic substrates, J. Mater. Process. Technol. 213 (2013) 1970–1977, https://doi.org/10.1016/j.jmatprotec.2013.05.011.

[15] Arduino Mega 2560 Rev 3, (n.d.). https://store.arduino.cc/usa/arduino-mega-2560-rev3.

[16] Pronterface, (n.d.). http://www.pronterface.com/.

[17] THORLABS, D5146-101S, (n.d.). https://www.thorlabs.com/thorproduct.cfm?partnumber=DL5146-101S.

[18] Y. Zhang, S. Ge, B. Tang, T. Koga, M.H. Rafailovich, J.C. Sokolov, D.G. Peiffer, Z. Li, A.J. Dias, K.O. McElrath, M.Y. Lin, S.K. Satija, S.G. Urquhart, H. Ade, D. Nguyen, Effect of Carbon Black and Silica Fillers in Elastomer Blends, Macromolecules 34 (2001) 7056–7065.

[19] Fumed Silica Powder (SiO2), (n.d.). http://www.reade.com/products/fumed-silica-powder-sio2.

[20] Sonics and Materials Inc UltrasonicHomogenizer, (n.d.). https://www.sonics.com/liquid-processing/.

[21] T. Mahrholz, J. Stängle, M. Sinapius, Quantitation of the reinforcement effect of silica nanoparticles in epoxy resins used in liquid composite moulding processes, Compos. Part A Appl. Sci. Manuf. 40 (2009) 235–243, https://doi.org/10.1016/j.compositesa.2008.11.008.

[22] H.-Y. Liu, G.-T. Wang, Y.-W. Mai, Y. Zeng, On fracture toughness of nano-particle modified epoxy, Compos. Part B Eng. 42 (2011) 2170–2175, https://doi.org/10.1016/j.compositesb.2011.05.014.

[23] F.N. Ahmad, M. Jaafar, S. Palaniandy, K.A.M. Azizli, Effect of particle shape of silica mineral on the properties of epoxy composites, Compos. Sci. Technol. 68 (2008) 346–353, https://doi.org/10.1016/j.compscitech.2007.07.015.

[24] S. Sun, C. Li, L. Zhang, H.L. Du, J.S. Burnell-Gray, Effects of surface modification of fumed silica on interfacial structures and mechanical properties of poly(vinyl chloride) composites, Eur. Polym. J. 42 (2006) 1643–1652, https://doi.org/10.1016/j.eurpolymj.2006.01.012.

[25] M.F. Uddin, C.T. Sun, Strength of unidirectional Glass/Epoxy composite with silica nanoparticle-enhanced matrix, Compos. Sci. Technol. (2008) 1637–1643.

[26] J. Jiao, X. Sun, T.J. Pinnavaia, Mesostructured silica for the reinforcement and toughening of rubbery and glassy epoxy polymers, Polymer (Guildf) 50 (2009) 983–989, https://doi.org/10.1016/j.polymer.2008.12.042.

[27] C. Chen, R.S. Justice, D.W. Schaefer, J.W. Baur, Highly dispersed nanosilica–epoxy resins with enhanced mechanical properties, Polymer (Guildf) 49 (2008) 3805–3815, https://doi.org/10.1016/j.polymer.2008.06.023.

[28] J.-L. Tsai, H. Hsiao, Y.-L. Cheng, Investigating mechanical behaviors of silica nanoparticle reinforced composites, J. Compos. Mater. 44 (2010) 505–524, https://doi.org/10.1177/0021998309346138.